SHIPBOARD MEASUREMENTS OF 0.6328 MICROMETER LASER BEAM EXTINCTION IN THE MARINE BOUNDARY LAYER

P. W. Parish

NAVAL POSTGRADUATE SCHOOL
Monterey, California

THESIS

SHIPBOARD MEASUREMENTS OF 0.6328
MICROMETER LASER BEAM EXTINCTION
IN THE MARINE BOUNDARY LAYER

by

P. W. Parish

June 1976

Thesis Advisor: G. W. Rodeback

20. Abstract (cont'd)

intensity monitor. Several calibration trials and three over-water experiments were conducted. A value on the order of 5×10^{-4} meters $^{-1}$ was found for the extinction coefficient in clear weather.

Shipboard Measurements of 0.6328 Micrometer Laser Beam Extinction in the Marine Boundary Layer

by

P. W. Parish
Lieutenant Commander, United States Navy
B.S., University of Nebraska, 1966

Submitted in partial fulfillment of the
requirements for the degree of

MASTER OF SCIENCE IN PHYSICS

ABSTRACT

A method of measuring laser beam extinction in the atmosphere over the ocean has been devised and satisfactorily utilized. An attempt has been made to correlate the observed values with existing meteorological conditions. The apparatus consisted of equipment, already being utilized for scintillation measurements, modified by the addition of a source intensity monitor. Several calibration trials and three over-water experiments were conducted. A value on the order of 5×10^{-4} meters $^{-1}$ was found for the extinction coefficient in clear weather.

TABLE OF CONTENTS

LIST OF FIGURES

I. PROBLEM DESCRIPTION

A. GENERAL

The increasing utilization of laser technology in long-range applications such as communications links, weapons designators/range finders, and high energy laser weapons makes it desirable to have the capability of predicting the effectiveness of the particular device at the termination of the path through the atmosphere. A highly collimated beam of monochromatic light, such as laser light, is affected by many phenomena among which scintillation, beam wander, beam spread, and attenuation are only a few. The development of a procedure by which the latter, commonly called extinction, could be measured in a path through the atmosphere directly above the ocean surface was the goal of this experiment.

Atmospheric attenuation (extinction) is generally caused by two phenomena: absorption by the gaseous molecules, and scattering by haze, fog, rain, and other aerosols. The absorption problem is minimized during system design by selecting a lasing medium that produces light of the proper wavelength so as to be within one of the several

transmission "windows" in the atmosphere. Thus, the degree of extinction becomes a function of the meteorological conditions.

Ideally, when sufficient data has been obtained, a system operator would only have to observe the existing meteorological conditions and thus predict the effectiveness of his equipment. Extinction measurements over terrain have previously been made [Ref. 1]. However, such measurements over the marine boundary are virtually non-existent.

B. MATHEMATICAL DESCRIPTION

If a beam of monochromatic flux enters an attenuating layer, the Bouger-Lambert Law [Ref. 2] states that the flux at any point within the layer is given by

$$P = P_o e^{-\mu x} \tag{1}$$

where P = Flux remaining after the beam has traversed a path length x,

P_o = Flux entering the attenuating layer,

μ = Extinction Coefficient,

x = Path length in the attenuating layer.

The flux described in equation (1) above has the units of energy per unit time over a given area and will be further described.

Considering both absorption and scattering the extinction coefficient

becomes $\mu = \alpha + \gamma$ (2)

where α = absorption coefficient,

and γ = scattering coefficient.

In this experiment, 0.6328 micrometer wavelength laser light was utilized and since this is within one of the transmission "windows" no attempt was made to distinguish the relative values of α and γ, but only to determine their combined value.

The relationship (Equation 1) holds for a spherical wave. The detailed mathematical development, following references 3 and 4, presented in Appendix A, shows that a laser source producing pure monochromatic radiation can be considered to be a point source of spherical waves, provided the observations are made in the paraxial region, at a distance from the source much greater than the off-axis position.

Thus, considering again equation (1), and assuming that the effective source of the radiation is at the Gaussian waist of the diverged beam and radiates P_o watts into a solid angle Ω, then the intensity at a position near the beam axis at a distance R is given by

$$I = \frac{P_o\, e^{-\mu R}}{\Omega\, R^2}, \tag{3}$$

where I = Intensity at R in Watts/meter^2

$\Omega\, R^2$ = Area of beam at distance R.

Consider propagation in a controlled atmosphere where scattering aerosols are at a minimum, so that $\mu = \mu_o$, and a calibration factor can be determined from

$$I_o = \frac{P_o\, e^{-\mu_o R_o}}{\Omega\, R_o^2}, \tag{4}$$

where the subscript indicates all measurements taken during the controlled trial. Then from (4)

$$\frac{P_o}{\Omega} = I_o R_o^2\, e^{\mu_o R_o} \tag{5}$$

$$\text{so} \qquad I = \frac{I_o R_o^2\, e^{\mu_o R_o}\, e^{-\mu_o R_o}}{R^2} \tag{6}$$

Taking the Natural Logarithm results in

$$\ln (IR^2) = \ln (I_o R_o^2\, e^{\mu_o R_o}) - \mu_o R. \tag{7}$$

A plot of $\ln (IR^2)$ versus R will yield the ordinate intercept

$$\ln (I_o R_o^2\, e^{\mu_o R_o}) = \ln C. \tag{8}$$

So in general for longer ranges where the determination of μ is desired

$$I = \frac{C e^{-\mu R}}{R^2} \tag{9}$$

and $$\ln IR^2 = \ln C - \mu R \tag{10}$$

from which: $$\mu = \frac{\ln C - \ln IR^2}{R}. \tag{11}$$

Values of $\ln \{IR^2\}$ at each value of R can thus yield a calculated value of μ.

Alternatively, it is only necessary to plot $\ln \{IR^2\}$ versus R for a series of measurements at increasing ranges and from this determine μ as the absolute value of the slope. This assumes, of course, that μ remains constant over the time and distance of the measurements.

To obtain the necessary data for the plot of $\ln \{IR^2\}$ versus R the procedure briefly described below is followed:

A horizontally fanned beam of constant intensity sweeps vertically across a detector located at a known distance R, 4000 times each second. The peak value of each detected pulse is recorded and the pulse height distribution (spread out because of scintillation) is obtained. The average value of the pulse height is calculated and taken to be a measure of the average intensity I, at the distance R.

II. EXPERIMENTAL APPARATUS

A. GENERAL

Since the ultimate goal of the experiment was to measure the extinction coefficient over the marine boundary in conjunction with simultaneous meteorological measurements, the use of the Research Vessel ACANIA was necessary. Because of the limited availability of the ship's services, it was deemed desirable to test equipment and procedures thoroughly prior to actual shipboard measurements. This was accomplished first in the 120 meter long basement hallway of the Naval Postgraduate School's, Spanagel Hall. To accomplish this the laser source and scanning equipment (to be described in detail in the next section) were placed at one end of the hallway, and the detector and processing equipment were moved the length of the hallway in twenty meter increments.

When operation of the equipment in this controlled environment was deemed satisfactory the apparatus was reconfigured. The laser source and scanning equipment were mounted on a training and elevating mechanism in a two-wheeled trailer. The detecting and processing equipment was mounted in an instrumented bus (Fig. 1) which provided

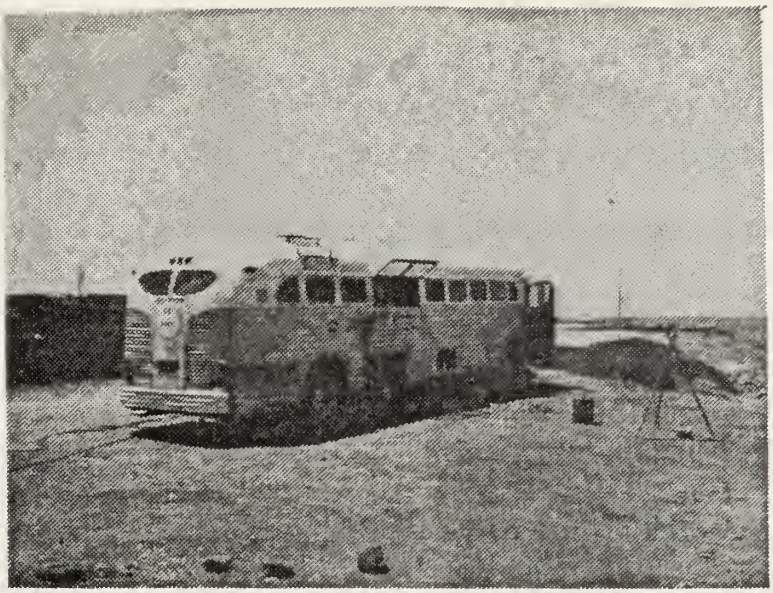

Naval Postgraduate School Mobile Optical Research Laboratory.

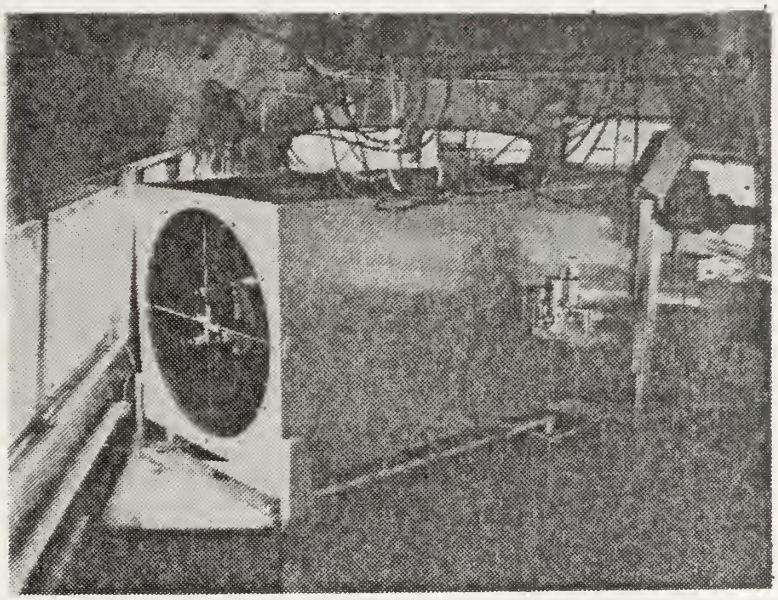

Interior, Showing 18-Inch Telescope.

FIGURE 1. INSTRUMENTED BUS and 18-Inch Telescope

portability, shelter, and 110 V.A.C. power from a 3.5 K.W. gasoline engine driven generator. This configuration provided the necessary support for extending the path length to 300 meters in 100 meter increments along O'HARE Avenue at the Naval Postgraduate School Annex. Operation in this manner was the final preliminary check prior to shipboard operation. For shipboard measurements the apparatus was again re-configured. The laser source and scanning equipment were mounted in the bus and the detecting and processing equipment were aboard ship. The reasoning behind this final re-configuration will become apparent in the following paragraphs.

B. DETAILS OF EXTINCTION EQUIPMENT

The laser source, scanning equipment, detection, and processing equipment utilized for extinction measurements were also utilized for scintillation and aperture averaging measurements; however, only that equipment in direct support of the extinction experiment will be described in detail.

1. Bus Mounted Equipment

Equipment described in the following paragraphs was mounted aboard the instrumented bus utilized by the optical propagation group. The bus itself was a converted

General Motors Corporation passenger bus. The forward one-third of the vehicle contained storage cabinets and workbench space and the drivers compartment. The after two-thirds of the vehicle contained electronic equipment racks, workbench, and an 18-inch telescope mounted on a platform capable of being raised clear of the floor on three hydraulic camper jacks extending through the floor to the ground. This arrangement provided a stable mount for the telescope and all equipment mounted on it and was thus isolated from any vibration caused by personnel moving about in the vehicle. A portable 3.5 kilowatt generator provided 110 V.A.C. power to all equipment.

a. Laser Source

The laser utilized as a source for the extinction measurements was a 0.6328 micrometer He-Ne laser manufactured by C.W. Radiation INC. The output of the laser was fitted with a diverging lens controlled by a micrometer screw adjustment. The laser, scanning equipment, and source intensity monitor were mounted on a common plate attached to the right-hand-side of the bus mounted 18-inch telescope (Fig. 1). This provided a means by which the laser could be trained, elevated, and aimed at the shipboard mounted detectors.

b. Scanning Equipment

(1) Physical Description. Mounted directly in front of the laser was a mirror positioned at a 45° downward angle (Fig. 2). This mirror performed two functions. First, it directed the beam down onto the scanning mirror. Secondly, it was capable of being bent, by means of a micrometer screw-adjustable knife-edge placed in the vertical axis, so as to produce a "FANNED" beam elongated in the horizontal plane. This arrangement was capable of producing a beam at the target ship sufficiently wide so as to provide uniform coverage of the detector as the ship moved and swung about its anchor.

The actual scanner consisted of a small, 1.0 cm x 1.0 cm, mirror mounted at a 45° upward angle [Ref. 6, p. 40]. This mirror, attached to two piano wires and mounted between the poles of a strong magnet, was set into oscillation and driven by a power amplifier. The amplifier controls were adjustable so as to provide a maximum vertical scan angle of 14 milliradians at a frequency of approximately 2000 HZ. The result of this beam processing was to allow detection of maximum intensity independent of the ship's vertical motion.

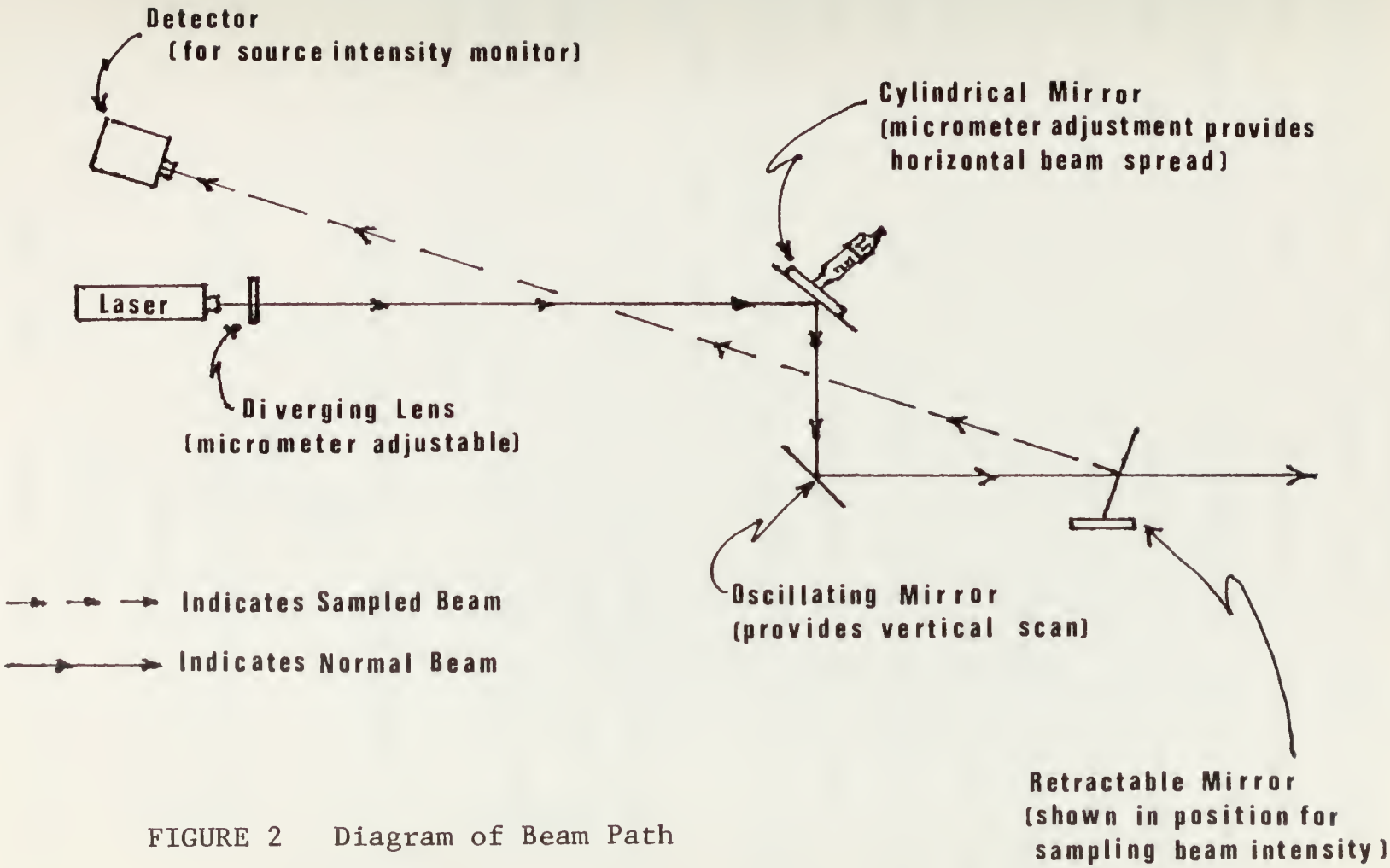

FIGURE 2 Diagram of Beam Path

(2) Mathematical Description. The following is a brief analysis of the scanned beam in terms of the vertical angular width of the beam and the scanning rate of the oscillating mirror. This permitted a prediction of the time width of the detected pulse which was then found to be in agreement with the measured value. To determine this the beam was fanned and both the unscanned and scanned beam sizes were measured at a convenient distance from the scanning mirror. Refer to Figure 3 for the details of the geometry; where ℓ (the distance from the scan mirror) = 2316.5 cm, h_1 (the unscanned beam height at ℓ) = 5.5 cm, and h_2 (the scanned beam height at ℓ) = 26 cm.

From this α , the unscanned beam angle of coverage, equals 2.37 milliradians and $2\theta_o$, the angle of coverage of the scanned beam, equals 11.22 milliradians. Thus, θ_o = 5.61 milliradians.

Now the pulse width τ is given by

$$\tau = \frac{\alpha + \beta}{\dot{\theta}_{max}} \tag{12}$$

where β = angle subtended at the scanning mirror by the detector,

and $\dot{\theta}_{max}$ = maximum angular scan rate.

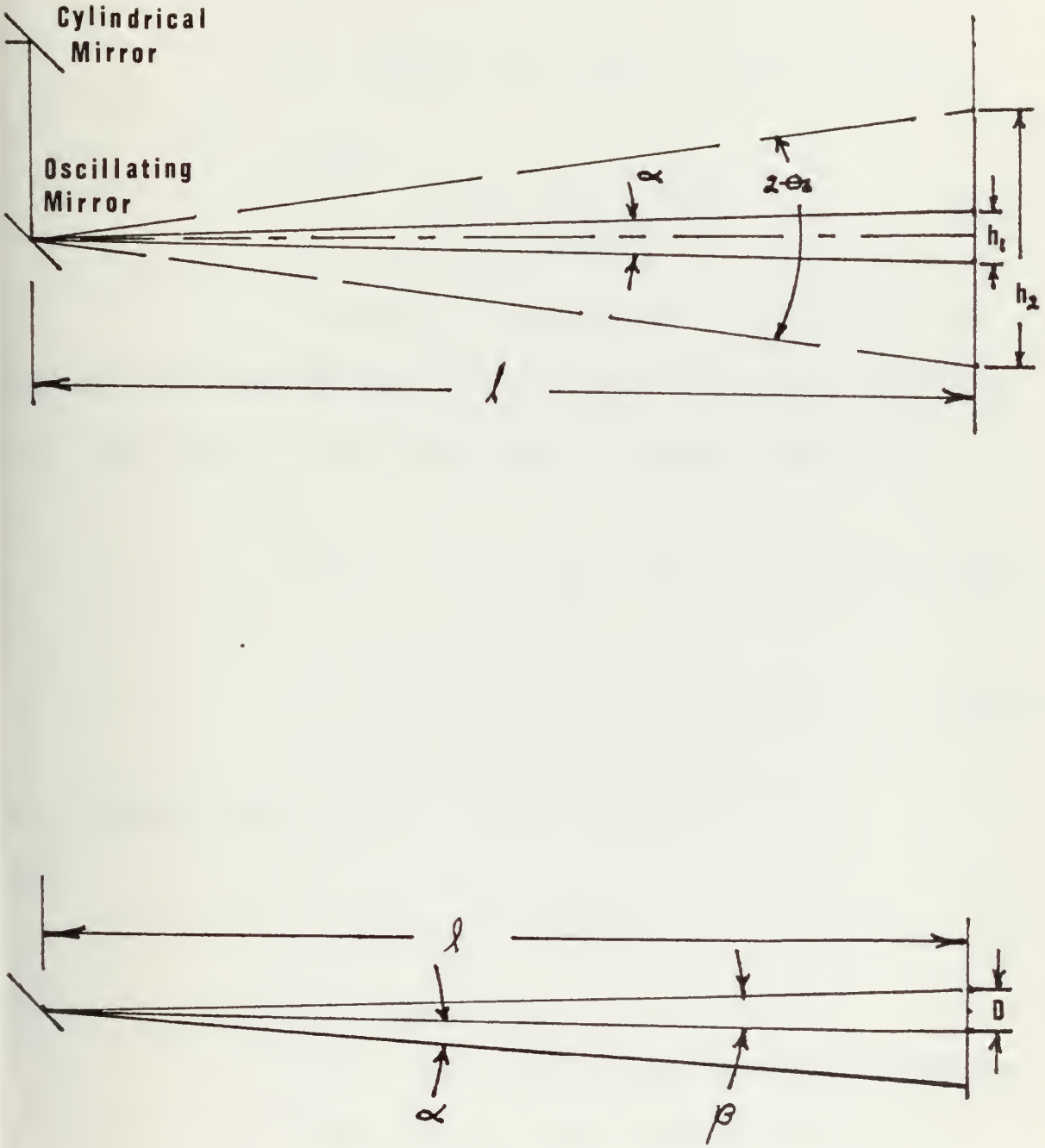

FIGURE 3 Geometry of Pulse Width Determination

Since $\beta \cong \frac{D}{\ell}$ for $\ell >> D$ where

D equals the height of the detector.

Thus,

$$\tau = \frac{\alpha + D/\ell}{\dot{\theta}_{max}} . \qquad (13)$$

For large values of ℓ, the second term in the numerator of (13) becomes negligible thus rendering the time width of the pulse nearly constant with range.

Now

$$\dot{\theta} = \frac{d}{dt} (\theta_0 \sin \omega t) , \qquad (14)$$

or

$$\dot{\theta} = \omega \theta_0 \cos \omega t. \qquad (15)$$

For maximum value of $\dot{\theta}$, $\cos \omega t = 1$

and

$$\dot{\theta}_{max} = \omega \theta_0 , \qquad (16)$$

with $\omega = 2\pi \times 2000$ Hz,

and θ_0 = 5.61 milliradians, as before;

Thus, $\dot{\theta}_{max}$ = 70.5 radians/sec.

For a detector of two centimeter diameter and ℓ as before, equation (13) yields a time width of the pulse, τ, of 45.8 microseconds. This agreed with oscilloscope measurements of the detected pulses.

Figure 4 shows the scanning equipment and mounting details; the entire assembly was referred to as the "FAN-SCAN."

c. Source Intensity Monitor

Periodically throughout the extinction measurements it was necessary to sample the laser output as the beam left the scanning mirror to ensure that no intensity degradation was present at the source. To facilitate this, the Source Intensity Monitor was devised (Fig. 4). An adjustable mirror was installed which could be swung into position to interrupt the outgoing beam and direct it back to the monitor detector mounted above and behind the source laser. The detector, a PIN-5D Photodiode was mounted in an adjustable mount to permit fine alignment of the sensitive surface with the sampled beam. The output of the detector was displayed on a Monsanto OS 226 P, oscilloscope.

2. Shipboard Mounted Equipment

The detection and signal processing equipment aboard the R.V. ACANIA included, detector, gyro-stabilized detector mount, PAR 113 Low-Noise Differential Preamplifier, Demodulator, Hewlett-Packard 7562A Log Voltmeter, Victoreen PIP-400 Multichannel Analyzer, and Hewlett-Packard HP 9810

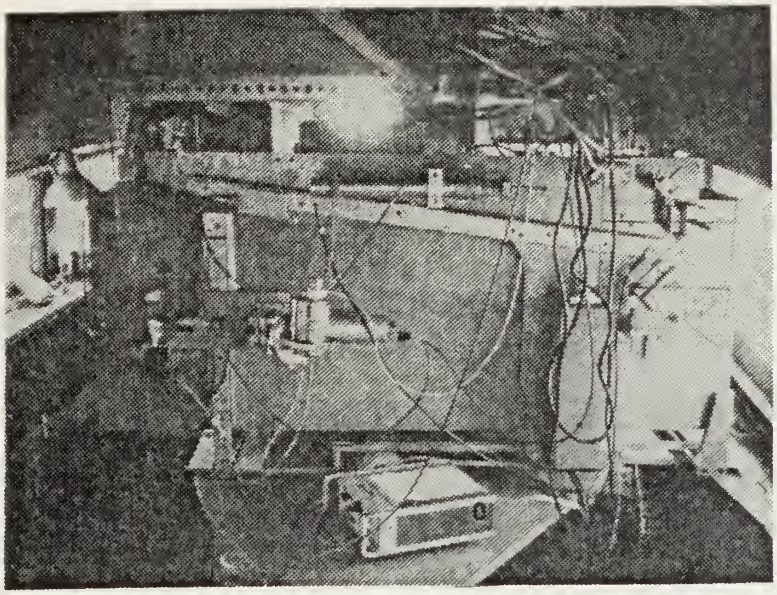

Laser Source and Scanning Equipment Mounted on 18-Inch Telescope.

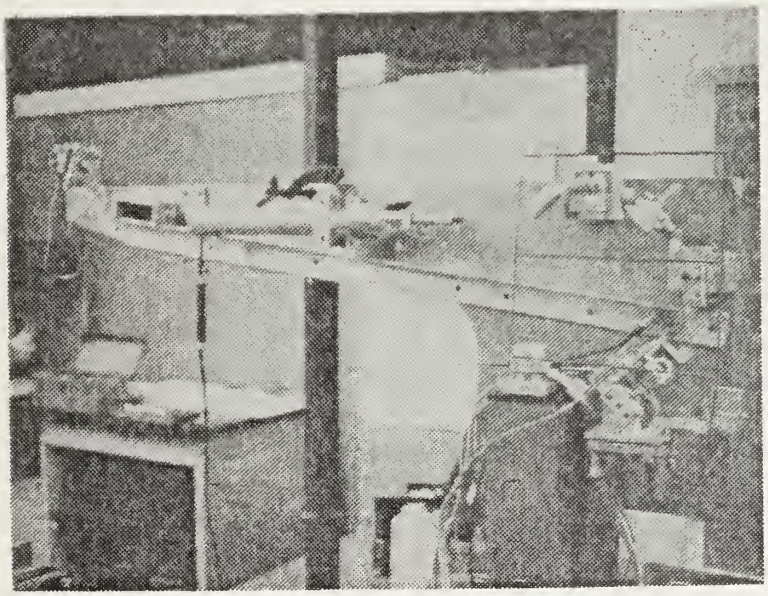

Close-up Showing, from left, Monitor Detector, Laser, Cylindrical Mirror, Oscillating Mirror, and Retractable Mirror.

FIGURE 4. "FAN-SCAN" and Source Intensity Monitor Arrangement

computer and associated plotter. The following paragraphs describe in detail the arrangement and function of each of the above.

a. Detector

The detector utilized for the extinction measurements was a TIX L69 Silicon Avalanche Photodiode reversed biased to 159 volts. This provided an acceptable Signal-To-Noise Ratio at the extended ranges. The detector was mounted in a holder fitted with lens and an aperture adjustable to 4.2 cm diameter. For more detailed discussion of the detector see [Ref. 7].

b. Gyro Stabilizer

The detector was mounted on the gyro stabilized mount. The stabilization was necessary to maintain alignment of the detector with the laser source ashore.

The gyro was an inertially stabilized platform utilizing two iron flywheels mounted on each end of a 1/2 hp capacitor start electric motor (Fig. 5). The shore based laser source utilized for the extinction measurements also served as the beacon onto which the gyro feedback circuit locked. Feedback was provided by a four-quadrant position and intensity photodetector with associated electronics.

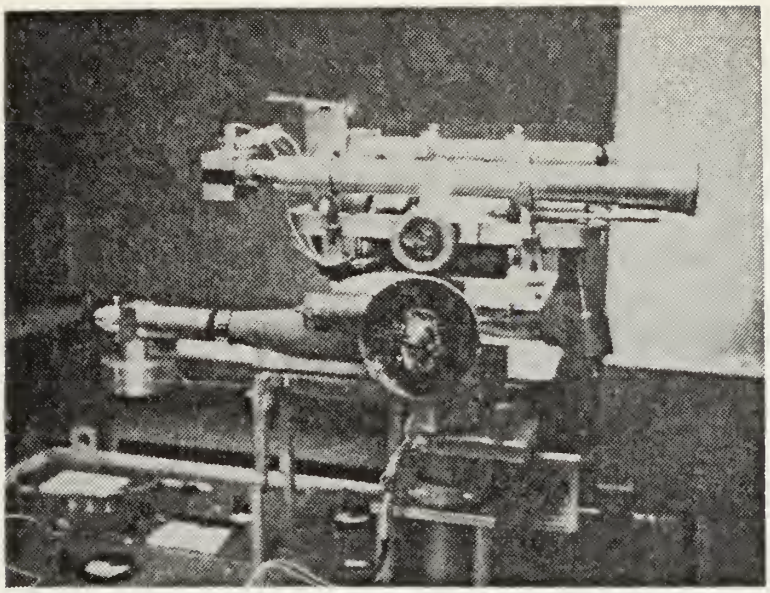

Gyro unit; showing top mounted Avalanche photodiode detector.

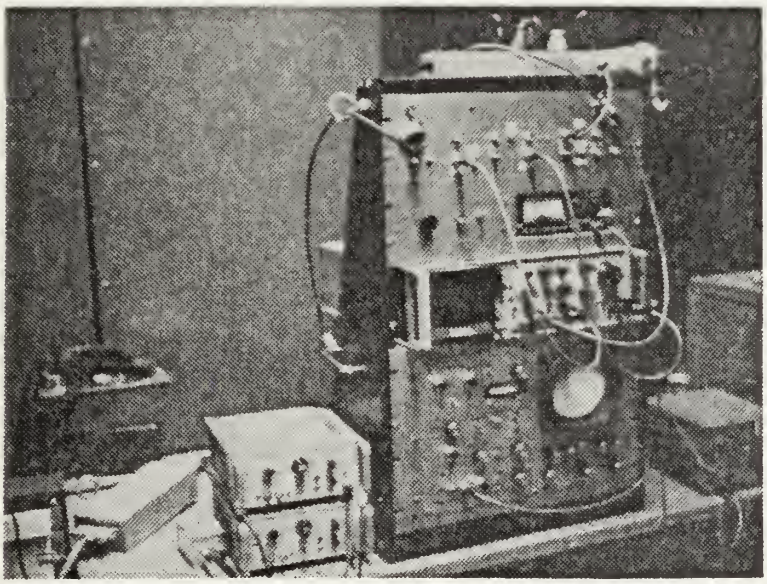

Signal processing equipment; PAR 113's(left); equipment in the rack (top to bottom); Demodulator, Log Voltmeter/Amplifier, Oscilloscope, and Multi-channel Analyzer.

Figure 5. Signal Detection and Processing Equipment

A small aiming telescope and "JOY STICK" control were mounted on the left side of the gyro to aid the gyro operator in aiming the control detector at the laser source. The gyro platform was positioned on the upper deck of ACANIA and was sheltered from the elements by an aluminum tool shed open on one side. The signal processing equipment described below was bench mounted in the "DRY LAB" on the main deck. (Fig. 5).

c. Preamplifier

The output of the detector was fed through an F.E.T. follower (which served the function of impedance matching) to the PAR 113 Low-Noise Preamplifier. This provided high gain, 10 to 10^4, low noise amplification, of the received signal. Adjustable High and Low Frequency Rolloffs allowed selection of the bandwidth.

d. Demodulator

The modulated signal was next passed to the Demodulator. This device sensed the scanning beam pulse, followed the pulse to its maximum and held that instantaneous signal level in a flat-topped pulse until the next maximum scanned across the detector at which time it held that maximum level, and so on. The output of this circuit was thus a series of step functions.

e. Log Voltmeter

The Hewlett-Packard 7562-A Log Voltmeter was the next instrument in the processing step. At this point the Logarithm of the signal was obtained.

f. Multichannel Analyzer

The Victoreen, PIP-400, Multichannel Analyzer collected, stored for further readout, and displayed the sampled Log Voltage Pulses. Each of the available 200 channels corresponded to a different pulse height and the number of pulses of any particular height received during the sampled period were stored in the respective channels.

g. Computer and Plotter

The output of the Multichannel Analyzer was fed into a Hewlett-Packard 9810A calculator. The calculator provided controlling functions to the associated plotter. The calculator sampled each channel of the Multichannel Analyzer, stored the information and plotted the pulse height distribution. The calculator then computed a least-squares polynomial fit of a Gaussian distributed curve to the data points. Using the position of this curve with respect to read-in calibration points and the Standard Deviation of the curve, the average intensity of the received signal was computed. See Appendix B for a detailed

analysis of the procedure for obtaining the average pulse height from the log voltage distribution. For a detailed description of the computer program see Ref. 8. Figure 6 is a sample printout from the system.

h. Humidity Measuring Equipment

The Hygrodynamics Digital I hygrometer indicator and the Dunmore-type Lithium Chloride sensor were used to measure the Relative Humidity. The equipment operates on the basis of resistance change within an electrolytic solution generating a reference voltage variance which is proportional to the relative humidity change. For further details see Ref. 9.

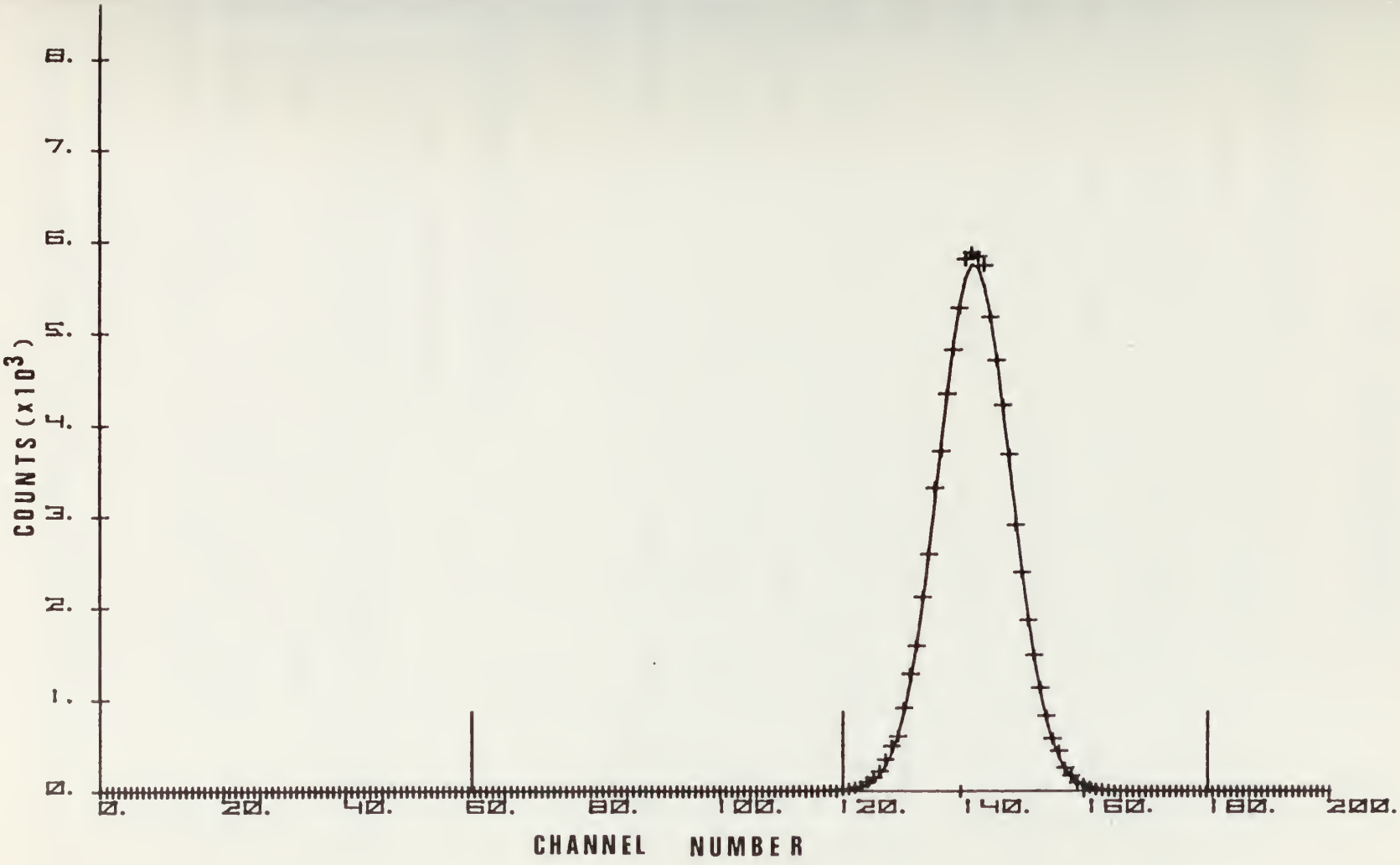

FIGURE 6 Sample Computer Output Showing "Best Fit" Gaussian Curve

III. THE EXPERIMENT

A. EXPERIMENTAL GOALS

The original goals of the experiment were threefold. First, the main goal was the development of the equipment and procedures to measure extinction and to demonstrate that extinction could be measured in the ocean environment. Secondly, it was desirable to correlate the observed extinction with the measured quantities of airborne particulate matter and water vapor measured as humidity. Thirdly, it was desired to measure the extinction caused by fog and rain. This last goal was not achieved since, during the scheduled shipboard trials, the weather was persistently clear.

B. EXPERIMENTAL PROCEDURE

1. 22-23 January 1976

On these dates the first equipment trials were performed in the basement hallway of Spanagel Hall, Naval Postgraduate School. The laser source and monitoring equipment were mounted on a portable equipment rack and positioned at distances of 15.8 m, 31.0 m, and 46.3 m from the receiving equipment which was kept stationary. The

purpose of these trials was to develop technique and initial equipment settings. At that time the signal detector was a PIN Photodiode which, for reasons to be explained in Section III.B.5, was replaced by the Avalanche Photodiode previously described. In addition to the development of techniques and equipment settings, these trials established the Laser Source Strength Monitor reference reading at 31 mv.

2. 26 January 1976

On this date the previous trials were repeated with similar results. In addition, the effects of "Fan-Scan" amplifier settings and PAR amplifier settings were measured. It was determined that "Fan-Scan" amplitude had a definite effect on the monitor pulse height and an amplifier setting of 1.2 was chosen as the best setting since the response at settings surrounding this point was relatively constant. The PAR settings arrived at were: (1) Low Frequency Rolloff 100 HZ, (2) High Frequency Rolloff 300 KHZ. These settings provided the cleanest signal response with minimum pulse shape distortion.

3. 2 February 1976

On this date, the first concrete attempt was made to determine the equipment response to transmission through

an atmosphere containing essentially no water droplets. The trial was again made in the basement hallway at transmission distances of 15.8 m, 31.0 m, 46.2 m, 61.5 m, 92.0 m and 122.5 m. All equipment settings were maintained as previously described; however, in this trial the laser source was left stationary and the detector and signal processing equipment were positioned at the prescribed ranges. This procedure was utilized since it facilitated more rapid detector alignment. The results of this trial are plotted in Figure 7. The observed value of $\ln \{IR^2\}$ determined here was to be utilized as $\ln \{C\}$ in the calculation of the extinction coefficient as a result of the data to be taken during the shipboard trials of the week of 29 March 1976.

4. 18 March 1976

It was decided that, prior to the 29 March Acania trip, it would be advantageous to have some measurements at longer distances than could be achieved in the basement hallway. For the calibration trial on this date the laser source and monitoring equipment was mounted in the small two-wheeled trailer, and positioned at the western end of O'Hare Avenue (NAVY ANNEX) in close proximity to the fuel station so that 115 volt A.C. power could be readily

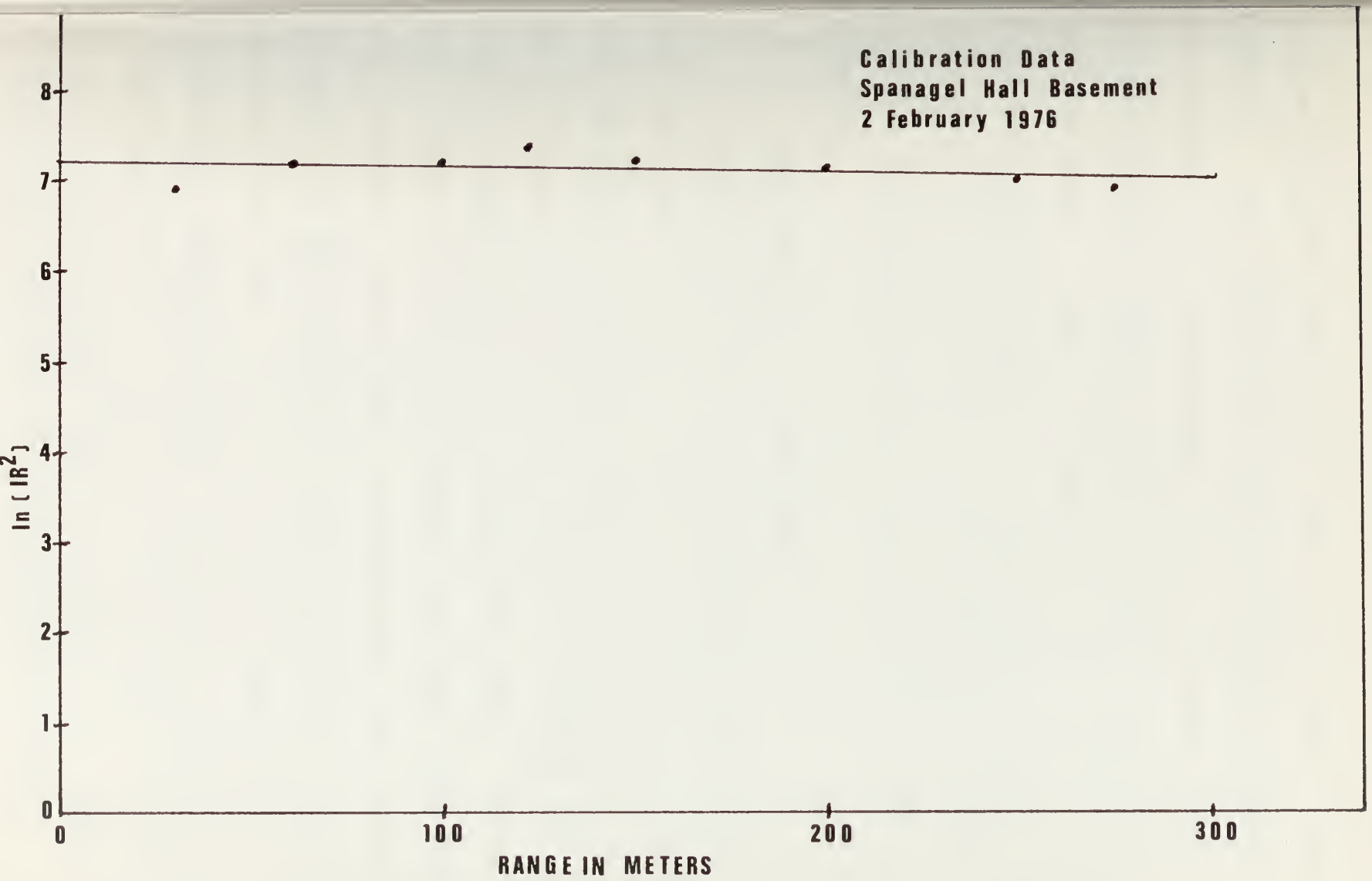

FIGURE 7 Graph of $\ln(IR^2)$ vs. R for 2 February 1976

obtained from the distribution panel located there. (See Figure 8). The detector and signal processing equipment was located in the instrumentation bus, which was moved and positioned at ranges of 91.0 m, 206.0 m, and 336.0 m from the source. (See also Figure 8). The results of this trial are plotted in Figure 9. These results together with the results of the 2 February trials were to be utilized with the data collected aboard Acania during the week of 29 March.

5. Week Beginning 29 March 1976

During this week, several extinction measurements were recorded aboard R. V. Acania. The majority were taken with the ship at anchor at a range of approximately 0.8 nautical miles off Point Pinos. Each day the ship would arrive on station and anchor using radar ranges. When the ship settled and rode to the anchor, the exact range from bus to ship was determined by triangulation using surveyor's transits. It was during this trial, on 30 March 1976, when an attempt was made to obtain extinction measurements at consistently increasing ranges, that it was determined that to do so would require the use of the Avalanche Detector; since, at ranges greater than two kilometers, the Signal-to-Noise Ratio obtained with the PIN Photodiode was

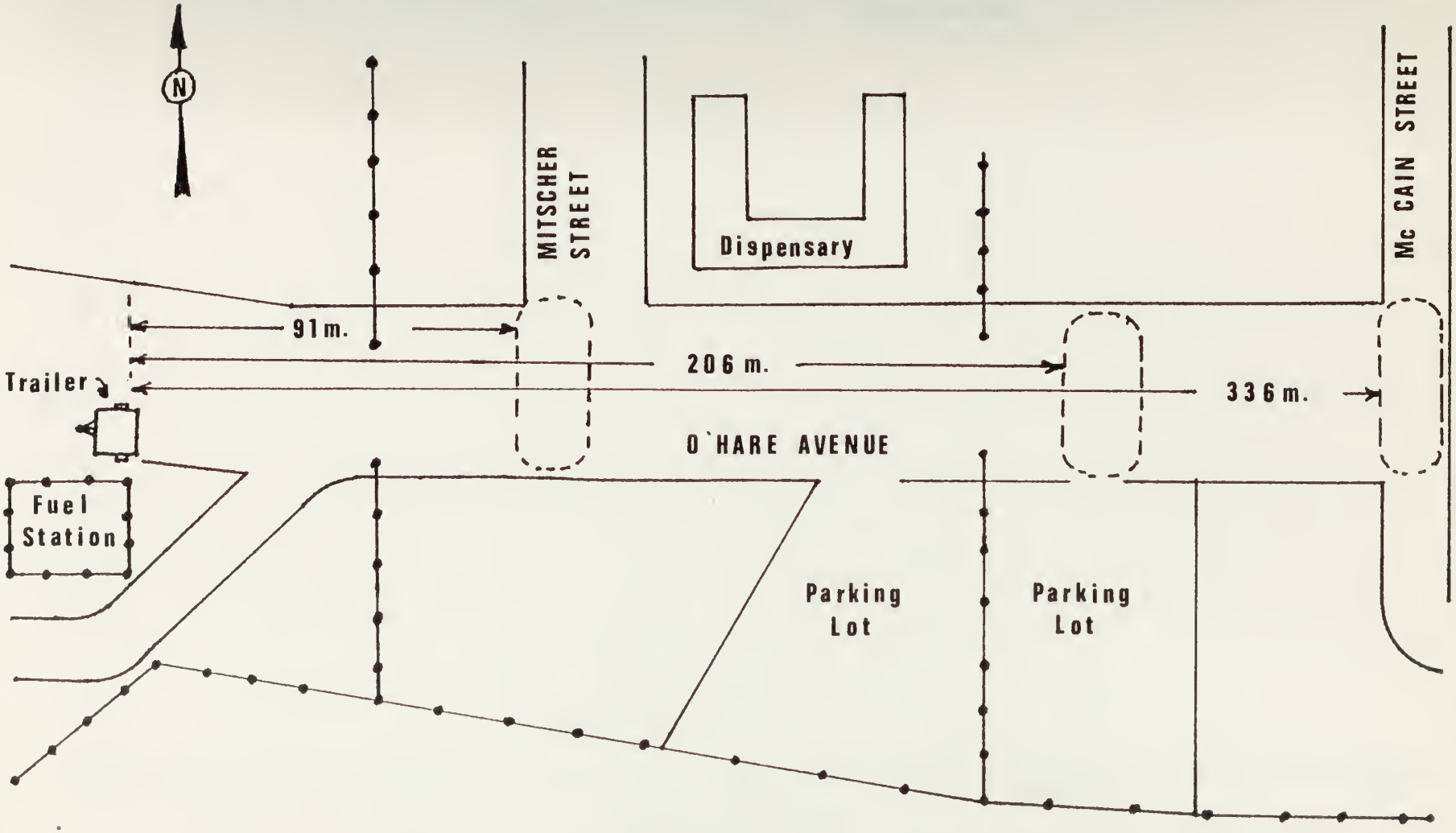

FIGURE 8 Drawing of Experimental Arrangement Naval Postgraduate School Annex

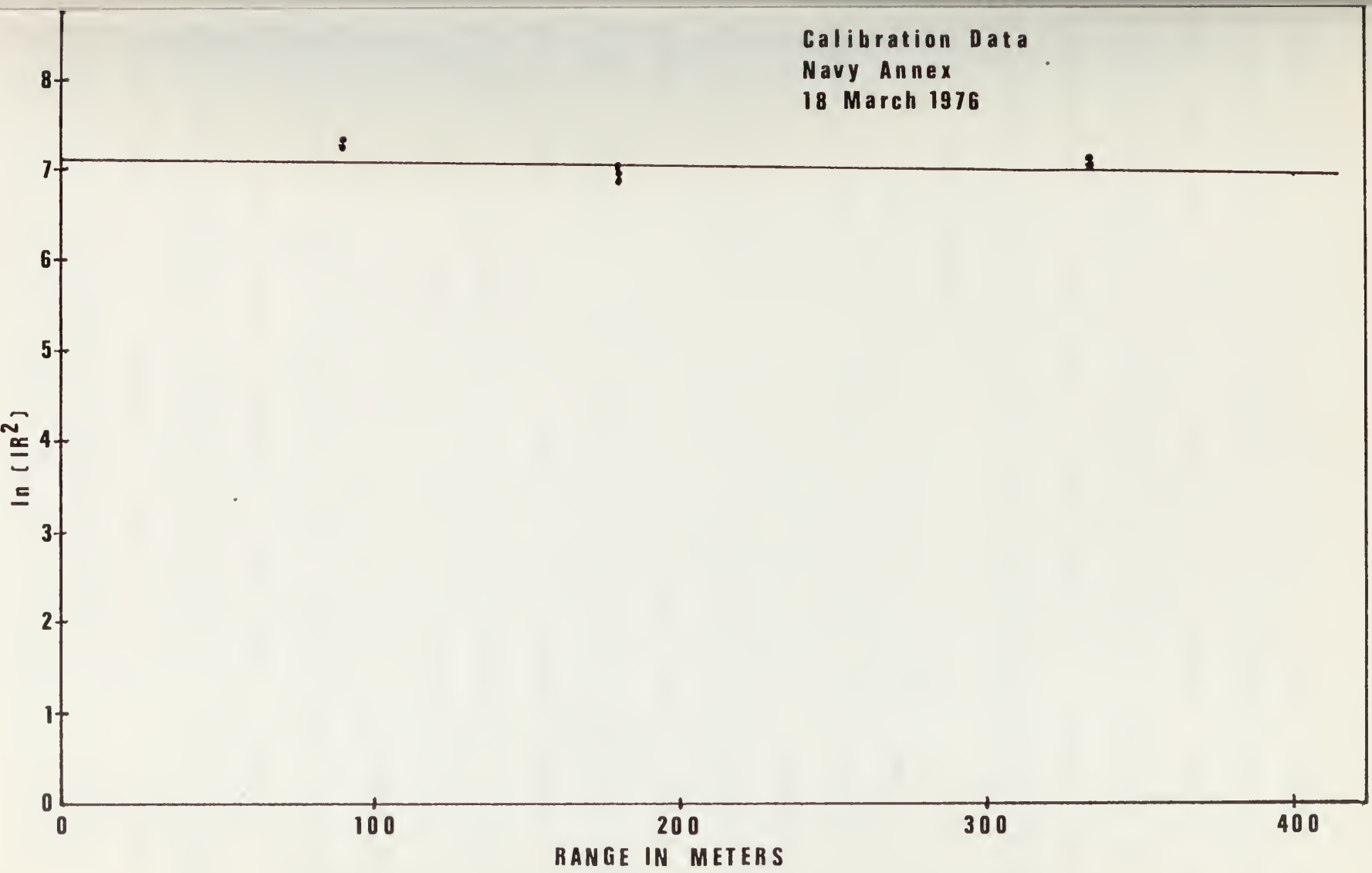

FIGURE 9 Graph of $\ln(IR^2)$ vs. R for 18 March 1976

insufficient. From this determination, it was decided that a "calibration" trial, similar to the 18 March trial, would have to be made using the Avalanche Photodiode. Since this detector produces an extremely large signal resulting in saturation at close ranges, it was decided to again work at the Navy Annex site rather than the Spanagel Hall basement.

6. 19-20 April 1976

On these dates the "calibration" trials were conducted utilizing the Avalanche Photodiode. The equipment was again configured as described previously in Paragraph 4. The source strength monitor at this time also produced a reading of 31 mv indicating that the laser output was remaining constant. The results of the trials described here are plotted in Figure 10. Again, the observed value of $\ln \{IR^2\}$ determined here was to be utilized as $\ln \{C\}$ in conjunction with the data to be collected during the final shipboard trials to be conducted the following week. Also, during this calibration trial, anticipating the need to use a large aperture opening at the longer ranges, a trial was conducted to determine the effect on the response of the detector as a function of aperture size. This was conducted at the longest available range (336.0 m) since opening the aperture greater than 0.4 cm diameter at the

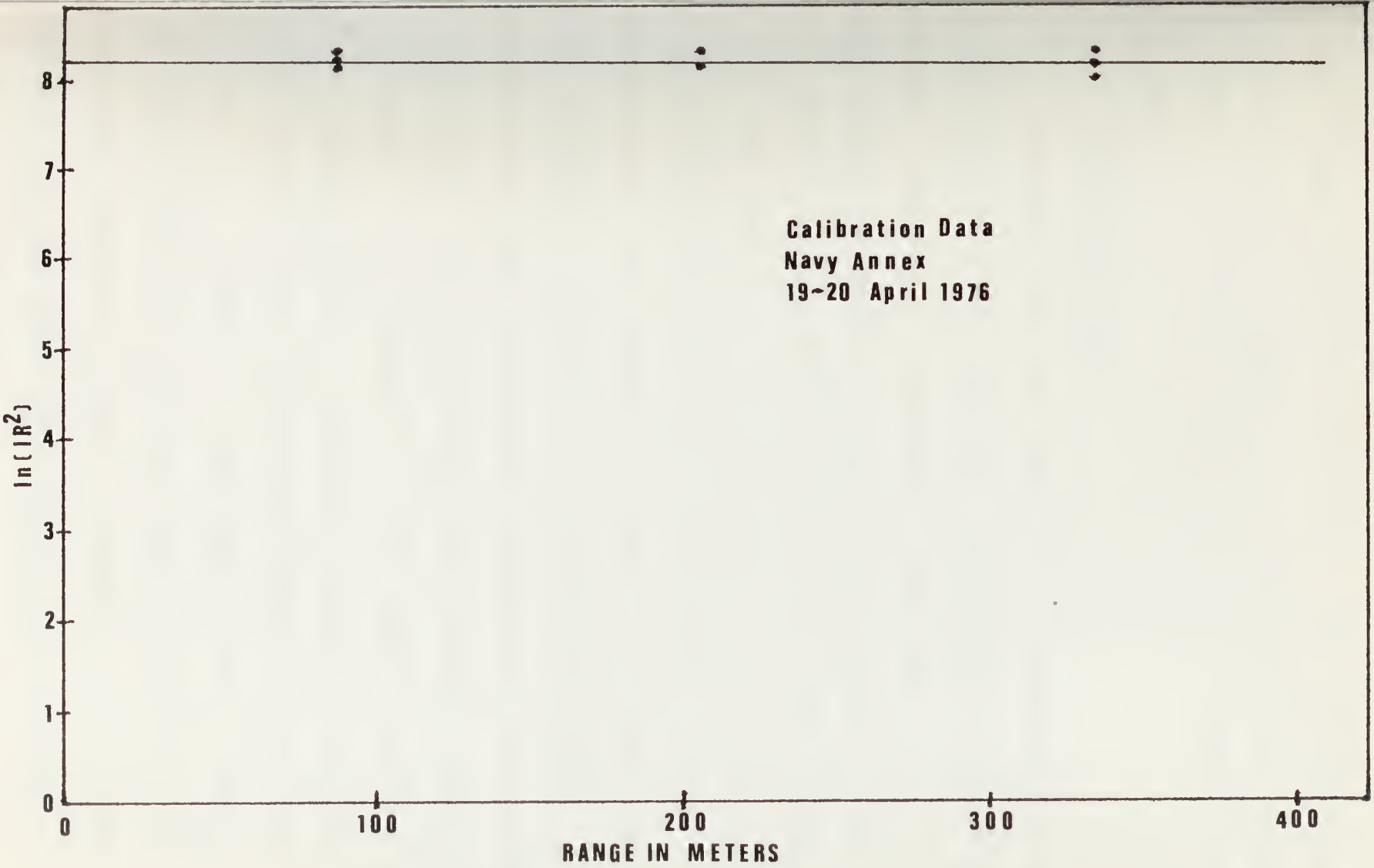

FIGURE 10 Graph of $\ln(IR^2)$ vs. R for 19-20 April 1976

closer ranges resulted in saturation. The results of this trial are plotted in Figure 11. As indicated the response is linear to an aperture radius of 1.1 cm, at which point saturation set in.

7. 28-29 April 1976

On these dates, the final data collection reported on in this thesis was completed. Simultaneous meteorological data was collected at the detector site aboard ship. The laser source was mounted on the 18 inch telescope in the bus. The bus was positioned at the water's edge on Point Pinos. The ship was positioned north of this location at various ranges from 839 meters to 6748 meters. Three factors arose that affected the effort to duplicate the exact equipment conditions of the calibration trials. First, because of the heavy electrical load on the 3.5 kw generator resulting in a low line voltage, the "Fan-Scan" amplifier setting had to be increased to 2.5 to maintain oscillation of the scanning mirror. Secondly, the source intensity monitor indicated some laser degradation as a result of the low voltage condition. The maximum monitor reading was 22.0 mv when the trial first began, then within 30 minutes of operation the monitor dropped to 18.5 mv and remained there throughout the remainder of the trials.

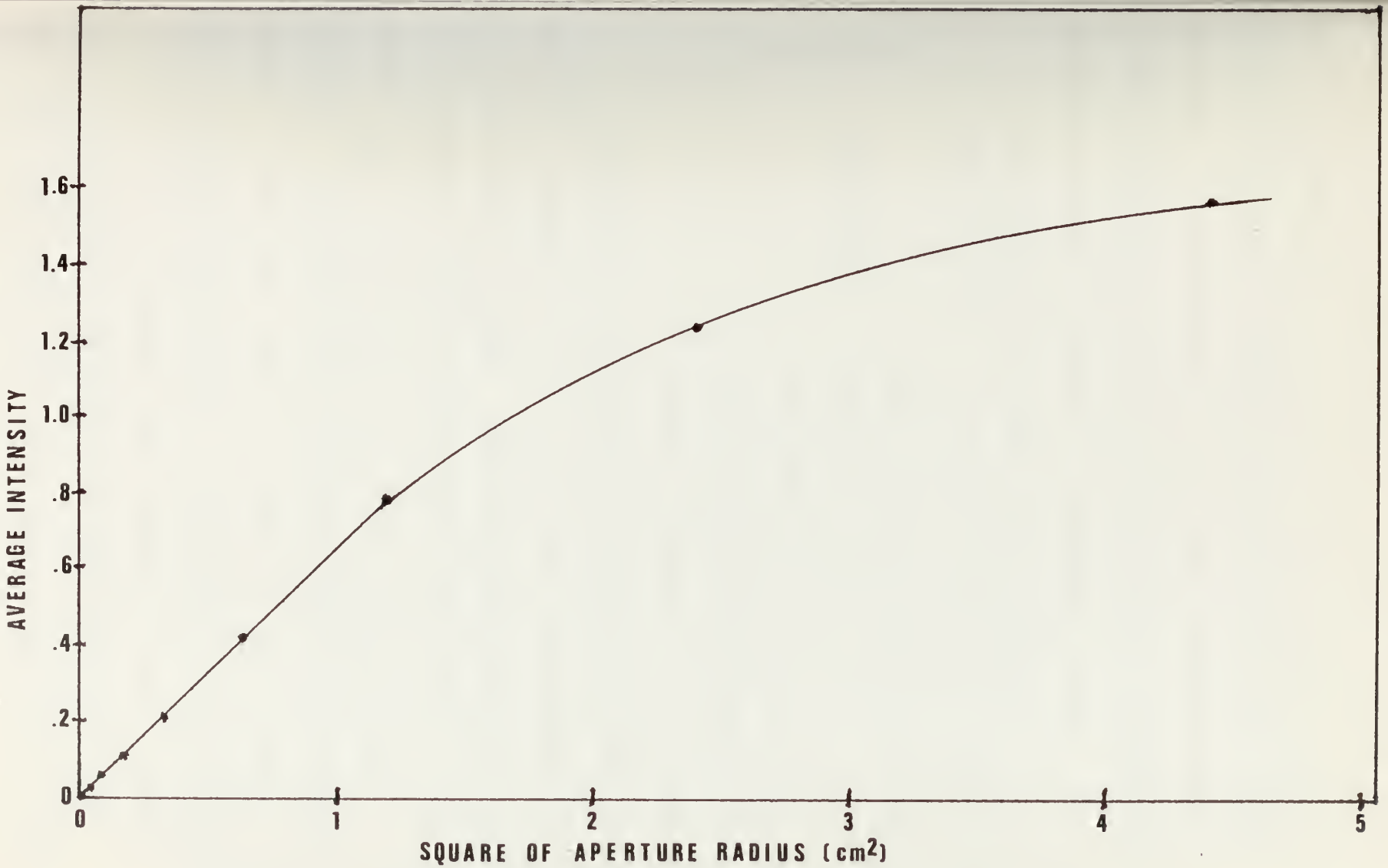

FIGURE 11 Graph of Average Intensity vs. Aperture Size

This was down from a constant 31.0 mv obtained during the calibration trials. Thirdly, because of the long ranges involved, it was decided that the best procedure would be to set the aperture size at 4.0 cm diameter and keep that constant setting throughout all remaining trials.

The equipment settings were as follows:

PAR Amplifier: Low Frequency Roll Off, 100 Hz.,
High Frequency Roll Off, 300 kHz;

"Fan-Scan": Amplifier, 2.5,
Cylindrical mirror micrometer, 7;
Laser divergence micrometer, 5;
Detector Aperture, 4.0 cm diameter.

The general experimental procedure for these two days was to maneuver the ship into position north of the bus at the desired range. When on station the gyro stabilized detector would be aimed at the laser source. When a usable signal was obtained the data collection would commence. The Multichannel Analyzer would be allowed to collect a sufficient number of counts so as to produce a nearly Gaussian distribution. This usually took from one to three minutes depending upon distance from the source. Since it was nearly impossible to hold the ship at the same range throughout data collection, approximately half

way through the collection process the ship's range from the source would be determined by triangulation with the surveyor's transits. As soon as the data collection was completed the ship would transit to the next desired position and the process would be repeated. While the ship was moving to the new position the data was fed into the HP 9810 Computer, processed, and plotted on the associated plotter; thus freeing the Multichannel Analyzer to collect data at the next position. At the closer ranges the gyro would "lock-on" the laser signal; however, at ranges greater than about 3000 meters the signal strength was not sufficient for "lock-on" thus the gyro operator controlled the aiming of the detector manually with the "Joy-Stick" control. The results of the data collected and the correction factors resulting from the equipment changes previously described are reported in Section IV, RESULTS AND CONCLUSIONS.

IV. RESULTS AND CONCLUSIONS

A. GENERAL

Since the major goal of the experiment, as stated earlier, was the determination of the extinction coefficient within the marine boundary layer, the actual data gathering revolved about the schedule of the Research Vessel Acania. Because of this and the discovery on 30 March of the long range limitations of the PIN Diode detector, the data breaks down logically into two distinct experimental evolutions: (1) the 30 March experiment and trials leading up to it, and (2) the 28-29 April experiment and the calibration trials leading to it.

To facilitate the determination of the extinction coefficient, μ, considering the paucity of long-range data, the Natural Logarithm of the quantity (IR^2) was plotted versus the range, R, for each data point obtained. A straight line was drawn through these data points utilizing the ordinate intercept and slope as determined from the Principle of Least Squares curve fitting [Ref. 10]. The absolute value of the slope of this curve is equal to μ, the extinction coefficient.

The calibration trials served to provide short-range data and thus determine, to a large degree, the ordinate intercept of the plot; whereas, the long-range data obtained in the desired ocean environment, from Point Pinos to Acania, provided the information for the slope and consequently μ.

Prior to plotting the data, the following corrections were made where necessary:

1. Source Intensity Correction

Since the majority of the data was taken with a laser source intensity monitor reading of 31.0 mv, the pulse height data taken while the laser intensity monitor reading differed from this was corrected either up or down according to the ratio of the two readings.

2. Aperture Size Correction

As mentioned earlier, it was necessary to utilize a small aperture at short ranges and a larger aperture at long ranges. Therefore, the data collected at the longer ranges was reduced by the ratio of the squares of the aperture radii.

B. THE 30 MARCH EXPERIMENT

The 30 March 1976 experiment and the calibration trials preceeding it served to establish the feasibility of making measurements at increasing ranges as well as providing the

initial measurement of the extinction coefficient in the marine environment. The data is tabulated in Appendix C. Figure 12 is the plotted data including the least squares fitted straight line. The weather was clear and the simultaneous meteorological observations provided an average relative humidity reading of 0.911 over the time of the shipboard measurements. μ was 6.2×10^{-4} meters $^{-1}$.

C. THE 28-29 APRIL EXPERIMENT

The experiments conducted on 28 and 29 April 1976, together with the preceeding calibration trials, succeeded in providing data at even longer ranges. The data taken on these two dates was considered together for calculation purposes because of the similar weather conditions and equipment operation. The data is tabulated in Appendix C. Figure 13 is the plotted data including the least squares fitted straight line. The weather was again clear and the relative humidity on 28 April was 0.776, while on 29 April it was 0.774 giving an average relative humidity reading of 0.775 over the time of the measurements. μ was 3.8×10^{-4} meters $^{-1}$.

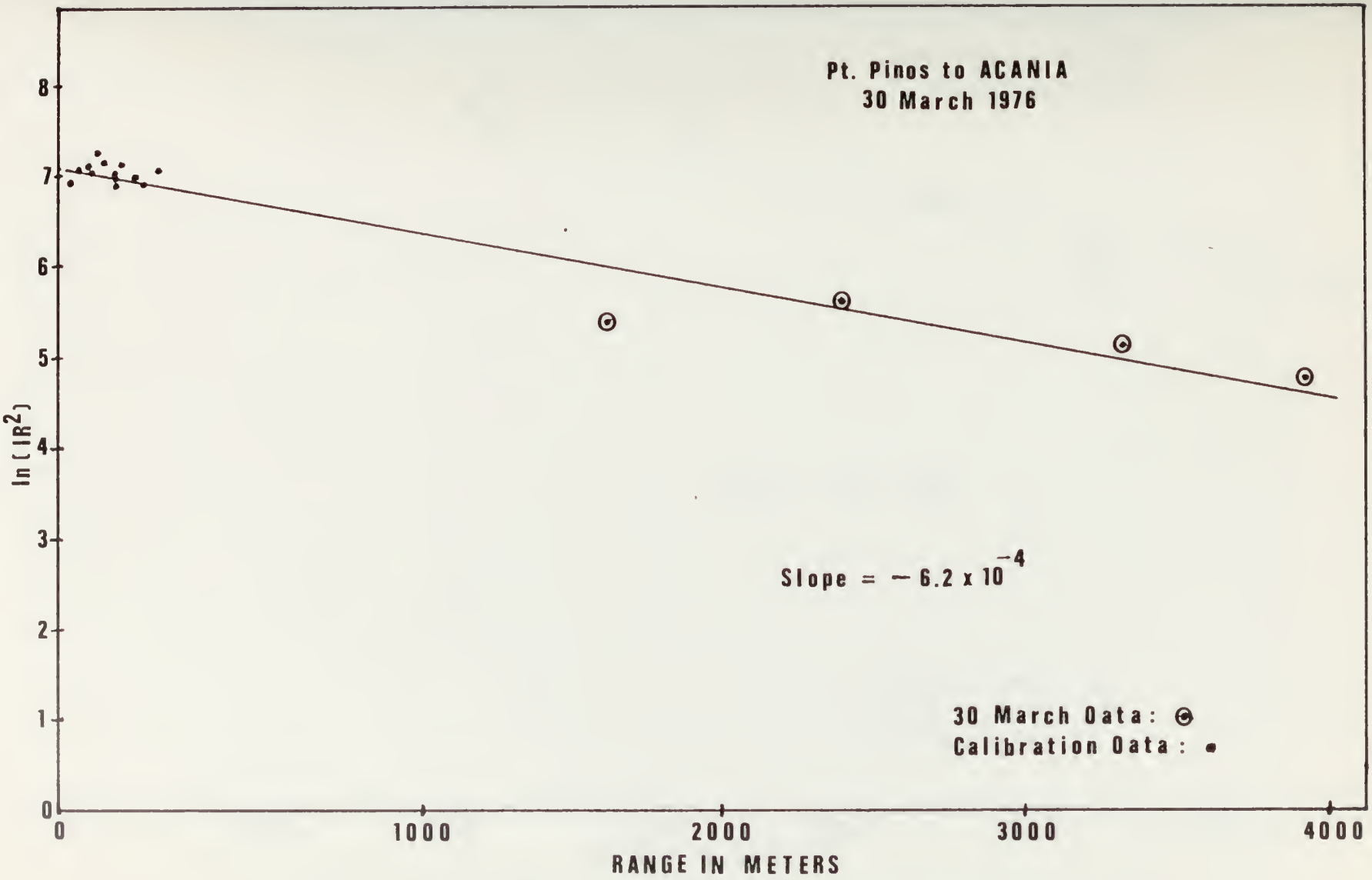

FIGURE 12 Graph of $\ln(IR^2)$ vs. R for 30 March 1976

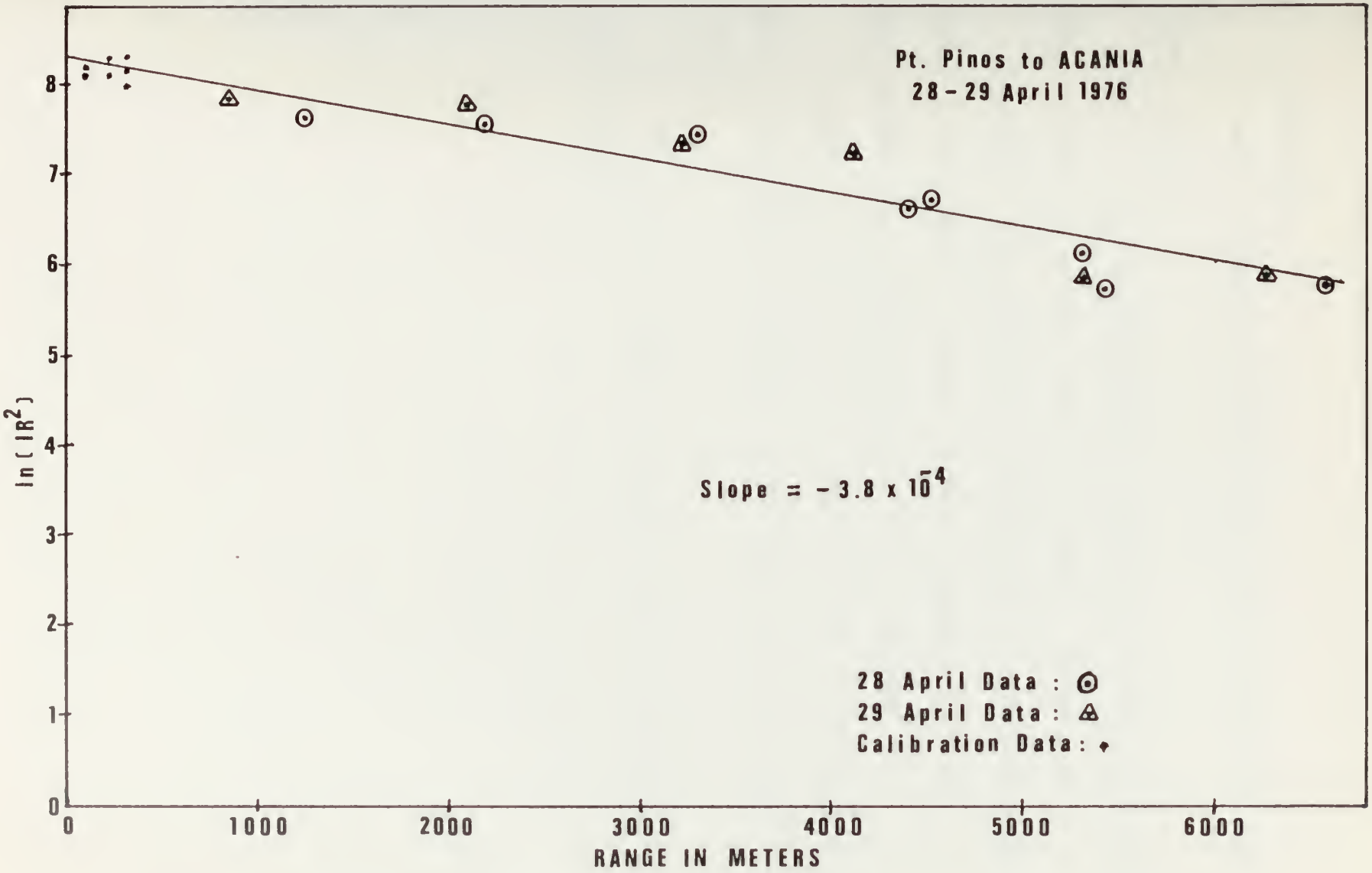

FIGURE 13 Graph of $\ln(IR^2)$ vs. R for 28-29 April 1976

D. CONCLUSIONS

It seems possible to draw three main conclusions from these results.

First, it is experimentally feasible to measure laser beam extinction at sea over the ocean-air interface.

Secondly, the extinction coefficient for 0.6328 micrometer laser light in clear weather, through the marine environment is of the order of 5×10^{-4} meters $^{-1}$.

Thirdly, humidity may be considered as a possible parameter with which to predict laser beam extinction in clear weather.

The latter two items, of course, require further investigation.

V. DISCUSSION OF ERRORS

The considerations and assumptions discussed below were utilized in an attempt to understand how the uncertainties in the measured quantities affect the uncertainty in the determination of μ .

$$I = \frac{C e^{-\mu R}}{R^2} \tag{17}$$

the more useful form

$$\ln \{ I R^2 \} = \ln C - \mu R, \tag{18}$$

was used. Then μ was determined to be the absolute value of the slope of the plot of ln IR^2 versus R. From (18)

$$\mu = \frac{\ln C - \ln I - 2 \ln R}{R} \tag{19}$$

From the theory of propagation of errors [Ref. 10];

$$(\Delta \mu)^2 = \left(\frac{\partial \mu}{\partial C}\right)^2 (\Delta C)^2 + \left(\frac{\partial \mu}{\partial I}\right)^2 (\Delta I)^2 + \left(\frac{\partial \mu}{\partial R}\right)^2 (\Delta R)^2. \tag{20}$$

From equation (19),

$$\frac{\partial \mu}{\partial C} = \frac{1}{RC} \quad , \quad \frac{\partial \mu}{\partial I} = -\frac{1}{RI}$$

and $\frac{\partial \mu}{\partial R} = -\left(\frac{2 + \mu R}{R^2}\right)$. Thus, the expression for

the relative error in μ becomes

$$\frac{\Delta\mu}{\mu} = \frac{\left[\left(\frac{\Delta C}{C}\right)^2 + \left(\frac{\Delta I}{I}\right)^2 + (2+\mu R)^2\left(\frac{\Delta R}{R}\right)^2\right]^{1/2}}{\mu R} \quad , \qquad (21)$$

where the uncertainties in C, I, and R are assumed to be independent. For the $\frac{\Delta R}{R}$ determination, two types of range error were assumed to exist; one because of ship drift during the time data was being collected, and the second because of surveying uncertainties. Therefore, $\frac{\Delta R}{R}$ becomes

$$\frac{\Delta R}{R} = \sqrt{\left(\frac{20}{R}\right)^2 + \left(\frac{0.05R}{6000}\right)^2} \quad , \qquad (22)$$

where $(\frac{20}{R})$ is the relative error introduced by assuming a 20 meter ship drift, and the $(\frac{0.05R}{6000})$ term arises from assuming a 300 meter error at 6000 meters and a lesser error as range decreases. Furthermore, it is assumed that $\frac{\Delta C}{C} = \frac{\Delta I}{I} = 0.05$, and a value of 5.0×10^{-4} is utilized for μ.

Then, utilizing equation (21), the above assumed values, and ranges from 1000 to 6000 meters in 1000 meter increments, a plot of the relative error versus range was constructed (Fig. 14).

In addition to the above investigation, the least squares calculations used in the curve fitting process were used to

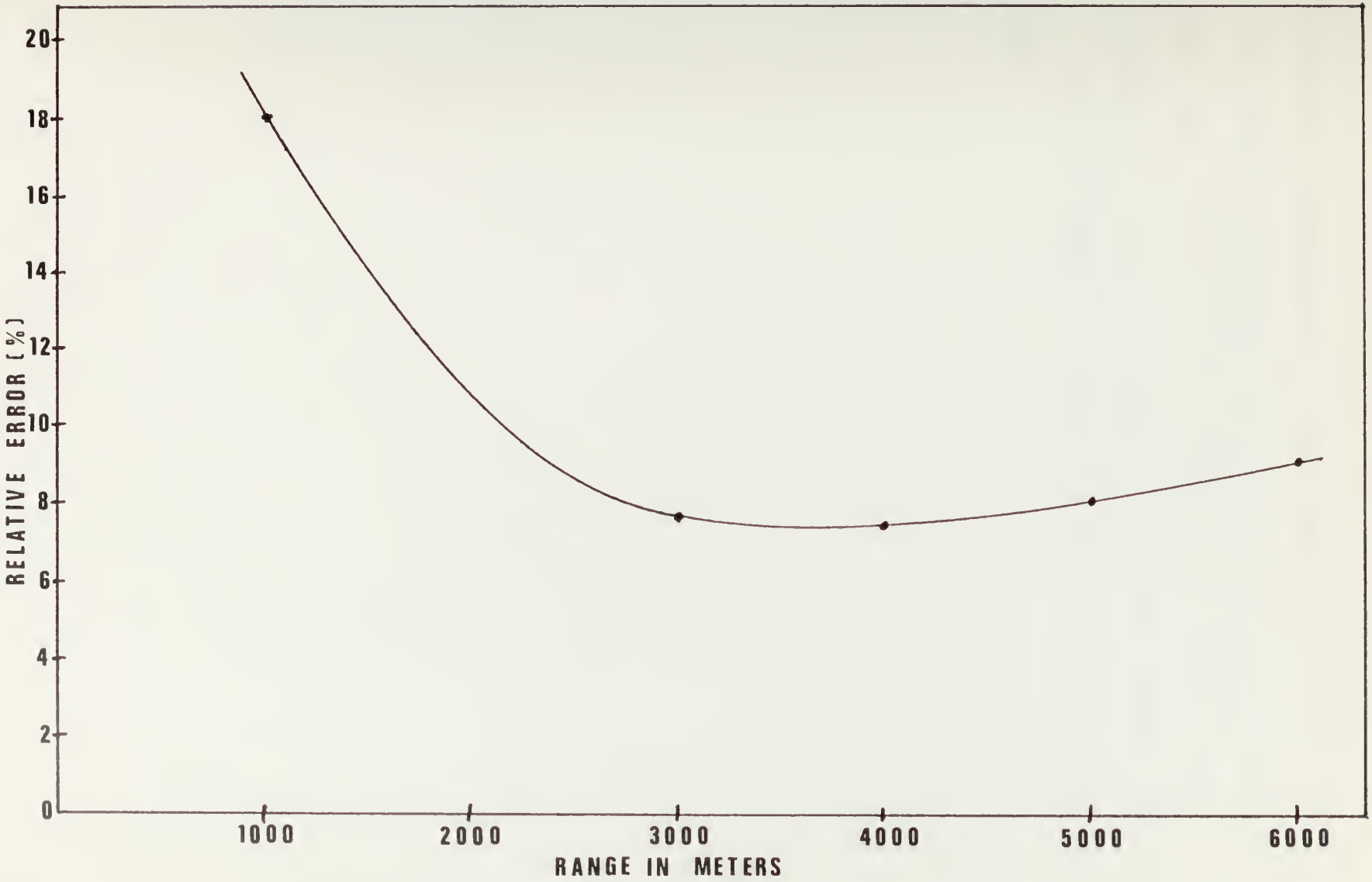

FIGURE 14 Graph of Relative Error vs. Range

determine the variance in the slope of the plotted data. The Standard Deviations of the data for 28 April and 29 April were found through separate calculations; the variance of each day's results were then computed.

This procedure indicated a relative error in μ of 16%.

VI. SUGGESTIONS FOR FURTHER INVESTIGATION

The following paragraphs are intended to present several ideas and modifications that, if implemented, would allow a more accurate determination of the extinction coefficient under the conditions experienced during this type of experiment. Furthermore, it would be possible to investigate the propagation of laser produced radiation at other wavelengths.

A new scanning device, recently procured, should serve to stabilize the "Fan-Scan" output under varying line voltage conditions.

A second demodulator unit, presently under construction, will provide an input to a digital voltmeter, thus facilitating a more accurate and rapid determination of the laser source intensity. Additionally, a method of monitoring the signal detection equipment performance would prove valuable.

The use of a Laser Rangefinder should be considered. This would provide more accurate and rapid source-to-detector range determination.

Ship to ship, or ship to some other waterborne platform, operations should be considered. Since the shoreline, across

which the propagation path passes in the present experimental setup, is rock strewn and relatively unprotected, waves breaking on these rocks produce a significant amount of airborne water particles and vapor. This being directly in front of the source can only act to produce a fallacious result in the determination of extinction. An experiment conducted entirely over water would eliminate this problem.

Further attempts should be made to measure 0.6328 micrometer radiation extinction in fog, mist, and rain. Also, an effort should be made to measure the extinction coefficient of other wavelength laser radiation; specifically, CO_2 produced, 10.6 micrometer radiation.

APPENDIX A

SPHERICAL WAVE SOLUTION TO THE WAVE EQUATION

The following development will show that a laser, which produces pure monochromatic radiation, can be considered to be a point source of spherical waves as long as the region of observation of these waves is restricted to a region near the beam axis and at a range from the source much greater than the distance off the axis.

Consider now a laser source in which the intensity distribution at planes normal to the propagation is Gaussian. Starting with the Maxwell Equations in a homogeneous charge-free medium, so that $\nabla \cdot \vec{E} = 0$, the characteristics of the Gaussian Beam are developed [Ref. 3].

Then $$\nabla \times \vec{H} = \epsilon \frac{\partial \vec{E}}{\partial t} + \vec{J} \quad , \tag{A-1}$$

Where $$\vec{J} = \sigma \vec{E},$$

Also $$\nabla \times \vec{E} = -\mu \frac{\partial \vec{H}}{\partial t} . \tag{A-2}$$

Taking the curl of (A-2) and substituting (A-1) for $\nabla \times \vec{H}$ results in

$$\nabla \times (\nabla \times \vec{E}) = -\mu \frac{\partial (\nabla \times \vec{H})}{\partial t} = -\mu \left\{ \frac{\partial}{\partial t} \epsilon \frac{\partial \vec{E}}{\partial t} + \sigma \vec{E} \right\}, \tag{A-3}$$

and $$\nabla \times (\nabla \times \vec{E}) = -\mu\epsilon \frac{\partial^2 \vec{E}}{\partial t^2} + \mu\sigma \frac{\partial \vec{E}}{\partial t} , \qquad (A-4)$$

or $$\nabla^2 \vec{E} - \mu\epsilon \frac{\partial^2 \vec{E}}{\partial t^2} - \mu\sigma \frac{\partial \vec{E}}{\partial t} = 0 , \qquad (A-5)$$

where $$\nabla \times \nabla \times \vec{E} \equiv \nabla (\nabla \cdot \vec{E}) - \nabla^2 \vec{E} ,$$

and $$\nabla \cdot \vec{E} = 0 .$$

Assuming that the field quantities vary as $\vec{E}(x,y,z,t) = \mathrm{Re}\{\vec{E}(x,y,z)\, e^{i\omega t}\}$ - that is pure monochromatic radiation such as from a laser - the Wave Equation (A-5) becomes

$$\nabla^2 \vec{E} + k^2(\vec{r})\, \vec{E} = 0 , \qquad (A-6)$$

where $$k^2 = \omega^2 \mu \epsilon \left\{ 1 - \frac{i\sigma}{\omega\epsilon} \right\}$$

and (A-6) allows for the possible dependence of k on position $\vec{r}$. At this point the development is limited to the case in which $k^2(\vec{r})$ is given by

$$k^2(\vec{r}) = k^2 - kk_2 r^2 , \qquad (A-7)$$

where k_2 is some constant and $k = \frac{2\pi}{\lambda}$, where λ is the wavelength of a TEM (Transverse Electromagnetic) plane wave propagating in the medium. Considering the propagation of a nearly plane wave in which the flow of energy is

predominantly along the z axis and assuming a solution to (A-6) whose transverse dependence is on $r = \sqrt{x^2 + y^2}$ only. then ∇^2 in (A-6) can be replaced by

$$\nabla^2 = \nabla_t^2 + \frac{\partial^2}{\partial z^2} = \frac{\partial^2}{\partial r^2} + \frac{1}{r}\frac{\partial}{\partial r} + \frac{\partial^2}{\partial z^2} \qquad \text{(A-8)}$$

taking $\vec{E}$ as

$$\vec{E} = \psi(x, y, z)\, e^{-ikz}, \qquad \text{(A-9)}$$

equation (A-6) becomes

$$\nabla^2\psi(x,y,z)e^{-ikz} + k^2\psi(x,y,z)e^{-ikz} - kk_2r^2\psi(x,y,z)e^{-ikz} = 0, \qquad \text{(A-10)}$$

and operating on (A-10) with (A-8)

$$\nabla_t^2\psi - 2ik\psi' - kk_2r^2\psi = 0, \qquad \text{(A-11)}$$

where $\psi' = \frac{\partial \psi}{\partial z}$, and the assumption is made that the transverse variation is slow enough that

$$k\psi' >> \psi'' << k^2\psi.$$

Taking ψ in the form of

$$\psi = \exp\left\{-i\left[P(z) + \tfrac{1}{2}Q(z)r^2\right]\right\}, \qquad \text{(A-12)}$$

substituting into (A-11), and using (A-8) gives

$$-Q^2r^2 - 2iQ - kr^2Q' - 2kP' - kk_2r^2 = 0. \qquad \text{(A-13)}$$

If (A-13) is to hold for all r, the coefficients of the different powers of r must be equal to zero. Thus

$$Q^2 + kQ' + kk_2 = 0, \tag{A-14}$$

and $$p' = \frac{-iQ}{k} . \tag{A-15}$$

Now according to (A-7), if the medium is homogeneous, k_2 can be set equal to zero and (A-14) becomes

$$Q^2 + kQ' = 0. \tag{A-16}$$

Now if the function S(z) is introduced by the relation

$$Q = k \frac{S'}{S}, \tag{A-17}$$

It follows from (A-16) that $S'' = 0$ and $S' = a$ also $S = az + b$ so that from (A-17)

$$Q(Z) = k \frac{a}{az+b} . \tag{A-18}$$

Following Kogelnik, [Ref. 4], it will be advantageous to define a parameter q (z) where

$$q(z) = \frac{k}{Q(z)} = \frac{2\pi}{\Lambda Q(z)} . \tag{A-19}$$

Now (A-18) may be rewritten as

$$q = z + q_0 . \tag{A-20}$$

Equation (A-15) may now be rewritten as

$$P' = \frac{-i}{q} = \frac{-i}{z+q_0} , \tag{A-21}$$

and

$$P(z) = -i \ln\left(1 + \frac{z}{q_0}\right) , \qquad \text{(A-22)}$$

where the arbitrary constant of integration is chosen as zero, which amounts to fixing the phase of the final solution at zero. Substituting (A-20) and (A-22) into (A-12)

$$\psi = \exp\left\{-i\left[-i \ln\left(1+\frac{z}{q_0}\right) + \frac{k}{2(q_0+z)} r^2\right]\right\} . \qquad \text{(A-23)}$$

Taking the arbitrary constant of integration q_0 to be purely imaginary which leads to waves whose energy density is confined to a region near the Z axis, and re-expressing it as a new constant ω_0

$$q_0 = \frac{i\pi\omega_0^2}{\lambda} , \qquad \text{(A-24)}$$

where

$$\lambda = \frac{2\pi}{k} . \qquad \text{(A-25)}$$

Using (A-24) and the fact that

$$\ln(a+ib) = \ln\sqrt{a^2+b^2} + i \tan^{-1}\left(\frac{b}{a}\right),$$

the first term of (A-23) becomes

$$\exp\left[-\ln\left(1-i\frac{\lambda z}{\pi\omega_0^2}\right)\right] = \frac{1}{\sqrt{1+\frac{\lambda^2 z^2}{\pi^2\omega_0^4}}} \exp\left[i \tan^{-1}\left(\frac{\lambda z}{\pi\omega_0^2}\right)\right] . \qquad \text{(A-26)}$$

Substituting (A-24) into the second term of (A-23) and separating into real and imaginary parts

$$\exp\left[\frac{-ikr^2}{2(q_0+z)}\right] = \exp\left\{\frac{-r^2}{\omega_0^2\left[1+\left(\frac{\lambda z}{\pi\omega_0^2}\right)^2\right]} - \frac{ikr^2}{2z\left[1+\left(\frac{\pi\omega_0^2}{\lambda z}\right)^2\right]}\right\}. \quad \text{(A-27)}$$

Defining the following parameters

$$\omega^2(z) = \omega_0^2\left[1+\left(\frac{\lambda z}{\pi\omega_0^2}\right)^2\right], \quad \text{(A-28)}$$

$$R = z\left[1+\left(\frac{\pi\omega_0^2}{\lambda z}\right)^2\right], \quad \text{(A-29)}$$

$$\phi = \tan^{-1}\left(\frac{\lambda z}{\pi\omega_0^2}\right), \quad \text{(A-30)}$$

Combining (A-26) and (A-27) into (A-23), and utilizing the fact that $\vec{E}(x,y,z) = \psi(x,y,z)e^{-ikz}$ results in

$$\vec{E}(x,y,z) = \frac{\omega_0}{\omega(z)}\exp\left[-i(kz-\phi) - r^2\left(\frac{1}{\omega^2(z)} + \frac{ik}{2R}\right)\right] \quad \text{(A-31)}$$

Consider now the form of a spherical wave emitted by a point radiator placed at Z = 0 [Ref. 3]. It is given by

$$E \propto \frac{1}{R}\exp\left(-ik\sqrt{x^2+y^2+z^2}\right)$$

$$\propto \frac{1}{R}\exp\left(-ikz - ik\,\frac{x^2+y^2}{2R}\right), \quad \text{(A-32)}$$

provided that $X^2 + Y^2 << Z^2$, the paraxial limitation, is observed.

The last form of equation (A-32) follows where Z is equal to R, the radius of curvature of the spherical wave. Since $r^2 = X^2 + y^2$, equation (A-32) becomes

$$E = \frac{1}{R} \exp\left(-ikz - r^2 \frac{ik}{2R}\right). \qquad \text{(A-33)}$$

Now, comparing the form of equation (A-31) to that of (A-33), it can be seen that (A-31) is in the form of a spherical wave, provided the observer is in the paraxial region at a distance much greater than the off-axis distance, and also provided that $\frac{\pi z}{\pi \omega_0^2} >> 1$.

APPENDIX B

PROCEDURE FOR DETERMINING AVERAGE VOLTAGE, $\bar{v}$, FROM LOG VOLTAGE DISTRIBUTION

The following development will serve to illustrate the validity of taking the peak value of the nearly Gaussian Log voltage distribution, as modified by the standard deviation of the best fit Gaussian curve, to be a measure of the average observed voltage $\bar{v}$.

Let

$$y = K \ln \frac{v}{v_0} \tag{B-1}$$

where

y = channel number in multichannel analyzer,

v = voltage into the log voltage circuit,

$K = \dfrac{y_2 - y_1}{\ln \frac{v_2}{v_1}}$ (v_1 and v_2 known calibration voltages),

and

$$v_0 = \frac{v_2}{e^{y_2/K}} = \frac{v_1}{e^{y_1/K}} .$$

Now, define

$$x = y/K \tag{B-2}$$

So that

$$x = \ln \frac{v}{v_0} \tag{B-3}$$

and

$$dx = \frac{dv}{v} . \tag{B-4}$$

From (B-3) and (B-4),

$$v = v_0 e^x . \tag{B-5}$$

Now

$$P(v)dv = p(x)dx \tag{B-6}$$

where

$$\int P(v)dv = \int p(x)dx \tag{B-7}$$

Thus, the average voltage $\bar{v}$ can be expressed as

$$\bar{v} = \frac{\int P(v)\, v\, dv}{\int P(v)\, dv} , \tag{B-8}$$

or using (B-7),

$$\bar{v} = \frac{1}{c} \int P(v)\, v\, dv . \tag{B-9}$$

from (B-6),

$$\bar{v} = \frac{1}{c} \int v\, p(x)\, dx . \tag{B-10}$$

Substituting (B-5) into (B-10) for v results in

$$\bar{v} = \frac{1}{c} \int v_0 e^x p(x)\, dx . \tag{B-11}$$

Now assume

$$p(x) = A e^{-\frac{(x-x_p)^2}{2\sigma_x^2}} , \tag{B-12}$$

and replacing p(x) in (B-11) results in

$$\bar{v} = \frac{v_o A}{C} \int e^{-\frac{(x-x_p)^2}{2\sigma_x^2}} e^{x} dx, \qquad \text{(B-13)}$$

or

$$\bar{v} = \frac{v_o A}{C} \int e^{-\frac{[(x-x_p)^2 - 2\sigma_x^2 x]}{2\sigma_x^2}} dx. \qquad \text{(B-14)}$$

Expanding the exponential:

$$\frac{(x-x_p)^2 - 2\sigma_x^2 x}{2\sigma_x^2} = \frac{[x-(x_p+\sigma_x^2)]^2}{2\sigma_x^2} - x_p - \frac{\sigma_x^2}{2}. \qquad \text{(B-15)}$$

Replacing the exponent in (B-14) by (B-15) results in

$$\bar{v} = \frac{v_o A}{C} \int e^{-\frac{[x-(x_p+\sigma_x^2)]^2}{2\sigma_x^2}} e^{x_p + \frac{\sigma_x^2}{2}} dx. \qquad \text{(B-16)}$$

Since $e^{x_p + \frac{\sigma_x^2}{2}}$ is independent of x, it can be removed from under the integral, and recognizing that $A\int e^{-\frac{[x-(x_p+\sigma_x^2)]^2}{2\sigma_x^2}} dx$ is equal to C, from (B-7) and (B-12), equation (B-16) becomes

$$\bar{v} = v_o e^{x_p + \frac{\sigma_x^2}{2}}. \qquad \text{(B-17)}$$

In actual operation, p(x) was the distribution collected by the multichannel analyzer. In calculating the best Gaussian

curve fitted to the data distribution, the computer generated $\chi_p, \sigma_{\bar{x}}$, and subsequently $\bar{v}$. The validity of this result depends solely on how well the computed Gaussian actually fits the experimental distribution. This was indicated graphically by the curve drawn onto the data (see Figure 6).

Reference 8 describes the computer program in detail.

APPENDIX C

DATA

SPANAGEL HALL BASEMENT	2 February 1976
RANGE (meters)	$\ln(IR^2)$
31	6.89
62	7.15
100	7.15
122	7.31
150	7.20
200	7.15
250	6.95
275	6.80
NAVY ANNEX	18 March 1976
91	7.23
91	7.26
181	7.01
181	6.83
181	6.99
335	7.04
335	7.06

NAVY ANNEX	19-20 April 1976
RANGE (meters)	$\ln(IR^2)$
91	8.19
91	8.22
91	8.25
91	8.15
206	8.14
206	8.30
336	7.99
336	8.34
336	8.14

PT. PINOS to ACANIA	30 March 1976
RANGE (Meters)	$\ln(IR^2)$
1604	5.42
2384	5.69
3323	5.19
3915	4.74

PT. PINOS to ACANIA	28 April 1976
RANGE (meters)	$\ln(IR^2)$
1279	7.52
2195	7.53
3288	7.42
4420	6.60
4535	6.65
5332	5.75
5425	5.69
6748	5.81

PT. PINOS to ACANIA	29 April 1976
RANGE (meters)	$\ln(IR^2)$
839	7.82
2120	7.76
3251	7.36
*4156	7.35
5300	6.12
6283	5.89

*The following is an example of the calculations and corrections applied to the value of $\bar{v}$, obtained from

the pulse height distribution, to arrive at the value of $\ln (IR^2)$ tabulated in this Appendix. The particular data point used in this example was chosen, since all corrections possible were applied in the determination of $\ln (IR^2)$.

$$\ln \{IR^2\} = \ln \left\{ \frac{\text{Average voltage from pulse height distribution}}{\text{Pre-amplifier Gain Setting}} \times \frac{31 \text{ mv}}{\text{Monitor Reading}} \times \frac{0.04}{(\text{Aperture Radius})^2} \times (\text{Range})^2 \right\}$$

$$= \ln \left\{ \frac{0.538}{100} \times \frac{31}{18.5} \times \frac{0.04}{4} \times (4156)^2 \right\}$$

$$= \ln \{1557.1244\}$$

$$= 7.35$$

LIST OF REFERENCES

1. Daino, B., Galeotti, M., Sette, D., "Statistical Measurement of Atmospheric 6328-Å Attenuation Using a Sequential Laser Transmissometer," Applied Optics, V. 15, p. 996-998, April 1976.

2. Hudson, R. E., Infrared System Engineering, Wiley, 1969.

3. Yariv, Amnon, Introduction to Optical Electronics, Holt, Rinehart and Winston, Inc., 1971.

4. Kogelnik, H., "On the Propagation of Gaussian Beams of Light Through Lens-like Media Including Those With a Loss or Gain Variation," Applied Optics, V. 4, p. 1562-1569, December 1965.

5. Hecht, E., Zajac, A., Optics, Addison-Wesley, 1974.

6. Cole, O. R., Shipboard Measurements of Laser Beam Scintillation in the Marine Boundary Layer, M.S. Thesis, U. S. Naval Postgraduate School, Monterey, 1974.

7. Hall, H. R., Aperture Averaging Effects on Scintillation and the Temporal-Frequency Power Spectrum, M.S. Thesis, U. S. Naval Postgraduate School, Monterey, 1976.

8. Plett, J. R., Pulse-Height Analyzer Interfacing and Computer Programming in the Environmental Laser Propagation Project, M.S. Thesis, U. S. Naval Postgraduate School, Monterey, 1976.

9. Hughes, M. M., An Investigation of Optically Relevant Turbulence Parameters in the Marine Boundary Layer, M.S. Thesis, U. S. Naval Postgraduate School, Monterey, 1976.

10. Parratt, L. G., Probability and Experimental Errors in Science, Dover Publications, Inc., 1961.

INITIAL DISTRIBUTION LIST

		No. Copies
1.	Defense Documentation Center Cameron Station Alexandria, Virginia 22314	2
2.	Library, Code 0212 Naval Postgraduate School Monterey, California 93940	2
3.	Professor K. E. Woehler, Chairman, Code 61Wh Department of Physics and Chemistry Naval Postgraduate School Monterey, California 93940	2
4.	Professor G. W. Rodeback, Code 61Rk Department of Physics and Chemistry Naval Postgraduate School Monterey, California 93940	2
5.	LCDR Philip W. Parish, USN Operational Test and Evaluation Force Pacific Staff Naval Air Station, North Island San Diego, California 92135	1

166407

Thesis
P1565
c.1

Parish

Shipboard measurements of 0.6328 micrometer laser beam extinction in the marine boundary layer.

166407

Thesis
P1565
c.1

Parish

Shipboard measurements of 0.6328 micrometer laser beam extinction in the marine boundary layer.